ADVANCES IN ATMOSPHERIC SCIENCES, VOL. 25, NO. 3, 2008, 367–379

Dynamical Tropopause Variability and Potential Vorticity Streamers in the Northern Hemisphere —A Climatological Analysis

Olivia MARTIUS*[1], Cornelia SCHWIERZ[2], and Michael SPRENGER[1]

[1] *Institute for Atmospheric and Climate Science, ETH Zurich,* 8092 *Zurich, Switzerland*

[2] *Institute for Atmospheric Science, School of Earth and Environment, Leeds University, Leeds LS2 9JT, UK*

(Received 2 February 2007; revised 8 June 2007)

ABSTRACT

This study presents a 44-year climatology of potential vorticity (PV) streamers in the Northern Hemisphere based upon analyses of the ERA-40 reanalysis data set. A comparison to an existing 15-year climatology yields very good agreement in the locations of PV streamer frequency maxima, but some differences are found in the amplitude of frequencies. The climatology is assessed with the focus on links between PV streamer frequencies and the synoptic- and planetary-scale variability of the dynamical tropopause.

A comprehensive overview is provided on where (zonally) and when (seasonally) short-term variability throughout the extra-tropical and sub-tropical tropopause is enhanced or reduced. Several key processes that influence this variability are discussed. Baroclinic processes, for example, determine the variability in the storm-track areas in winter, whereas the Asian summer monsoon significantly influences the variability over Asia.

The paper also describes links between the frequency of PV streamers in the extra-tropical and subtropical tropopause and three major northern hemisphere teleconnection patterns. The observed changes in the PV streamer frequencies are closely related to concomitant variations of PV and its gradient within the tropopause region. During opposite phases of the North Atlantic Oscillation the location of the streamer frequency maxima shifts significantly in the Atlantic and European region in both the extra-tropics and subtropics. The influence of ENSO on the streamer frequencies is most pronounced in the subtropical Pacific.

Key words: Rossby wave breaking, PV streamer, Northern Hemisphere teleconnection indices, dynamical tropopause

DOI: 10.1007/s00376-008-0367-z

1. Introduction

The spatial and temporal distribution in the local vertical position of the dynamical tropopause, defined by the 2-pvu (10^{-6} K kg^{-1} m^2 s^{-1}) isosurface, is constantly changing on synoptic and inter-annual time scales. In a composite potential vorticity (PV) and potential temperature depiction (Hoskins, 1991) this three-dimensional variability can be projected onto latitude versus pressure-level displays in the location of the dynamical tropopause. The first part of this study focuses on the annual cycle in the variability of the meridional position of the dynamical tropopause. The analysis is based upon a new 44-year climatology of the dynamical tropopause on isentropic surfaces.

It will be shown that areas of enhanced variability generally coincide with regions where stratospheric and tropospheric PV streamers frequently occur. PV streamers are meridionally elongated PV structures on isentropic surfaces with a narrow connection to the main stratospheric and tropospheric air masses, respectively (Appenzeller and Davies, 1992). Vertically the PV streamers are evident as up- and downward-vertical intrusions of stratospheric, high PV air into the troposphere (stratospheric PV streamers) or of tropospheric, low PV air into the stratosphere (tro-

*Corresponding author: Olivia MARTIUS, olivia@env.ethz.ch

pospheric PV streamers). Given their remarkable dynamical nature, PV streamers play a role in a number of relevant dynamical phenomena. These include: (1) the influence of PV streamers (i.e., local upper-level PV anomalies) on the evolution of surface weather systems (Hoskins et al., 1985) and on extreme weather events (e.g., Massacand et al., 1998; Martius et al., 2006b), (2) the link to air mass and pollutant exchanges across the dynamical tropopause (Sprenger et al., 2007), and (3) the forcing of subtropical and tropical convection (e.g., Matthews and Kiladis, 1999; Waugh and Funatsu, 2003; Knippertz and Martin, 2005). Changes in the location and frequency of PV streamers on an inter-annual time scale affect all of the above mentioned processes and are therefore of broad interest.

PV Streamers can be viewed as breaking synoptic-scale Rossby waves, a process that leads to an isentropic meridional redistribution of PV and PV gradients (Thorncroft et al., 1993; McIntyre, 2000 and references therein; Martius et al., 2007) and that is closely linked to the isentropic synoptic-scale variability of the tropopause. The rearrangement of PV in the tropopause region, that is associated with these breaking waves, projects well onto inter-annual variations of isentropic PV in that region tied to the North Atlantic Oscillation (Benedict et al., 2004; Franzke et al., 2004).

A second focus of this study is directed, therefore, toward links between PV streamers and three major Northern Hemisphere teleconnection patterns, the North Atlantic Oscillation (NAO), the El Niño-Southern Oscillation (ENSO) and the Pacific North American Pattern (PNA). These links are expected to be bidirectional. The basis for this is, first, the aforementioned observation that breaking synoptic-scale waves in the extra-tropics and the subtropics play a crucial role in the formation of the tropopause flow configuration during both the positive and the negative phase of the NAO (Benedict et al., 2004; Franzke et al., 2004; Abatzoglou and Magnusdottir, 2006). Second, from the reverse perspective, changes in the large-scale ambient flow that accompany opposite phases of the teleconnection patterns are expected to have a significant influence on the temporal and spatial distribution of PV streamers (e.g., Shapiro et al., 2001). Areas of weak, time mean PV gradients (i.e., weak jets) have been observed to coincide with an increased wave breaking activity (Postel and Hitchman, 1999). This can be understood in the framework of Rossby wave dynamics. The amplitude of synoptic-scale Rossby waves increases in areas where the PV gradient is weak, and strong amplification leads to wave breaking (e.g., Swanson et al., 1997; McIntyre, 2000).

In this paper links between PV streamers and the large-scale teleconnection patterns are explored using a new 44-year climatology of stratospheric and tropospheric PV streamers in the northern hemispheric extra-tropics and subtropics. The paper is structured as follows: The next section describes the data sets used, a brief introduction to the PV streamer detection method of Wernli and Sprenger (2007) is provided, and the ERA-15 and ERA-40 PV streamer climatologies are compared. The synoptic-scale variability of the dynamical tropopause on various isentropic surfaces is discussed in the third section. Section 4 is a discussion of the tropopause flow and the PV streamer characteristics during opposite phases of the three large-scale teleconnection patterns. Finally the results are summarized and discussed in section 5.

2. Data and method

2.1 *Isentropic tropopause and streamer identification*

In this study a novel method developed by Wernli and Sprenger (2007) is used to identify PV streamers on isentropic surfaces which transect the dynamical tropopause. The method allows identification of stratospheric, as well as tropospheric PV streamers. An extensive description of the algorithm, including various applications, can be found in Wernli and Sprenger (2007). Here, only a brief summary of the identification algorithm is provided.

The streamer climatology is derived from the ERA-40 data set (Uppala et al., 2005). The data fields are evaluated at six-hourly intervals and interpolated onto a $1^\circ \times 1^\circ$ grid. The PV streamers and the dynamical tropopause are identified on isentropic levels between 310 K and 360 K, with a 5 K vertical resolution. On these levels an objective identification algorithm (Wernli and Schwierz, 2006) detects the southern-most closed 2-pvu contour (i.e., dynamical tropopause) of the isentropic Ertel-PV field. Along this contour the PV streamers are identified as pronounced meridional excursions with a narrow connection between to the stratospheric and tropospheric main PV reservoirs. The identified features are flagged as stratospheric (tropospheric) streamers for southward (northward) excursions of the contour. The results are stored in a binomial field where all grid points inside the streamer area are set to one and the remaining grid points are set to zero. For the analysis of the streamer climatology, the six-hourly binomial fields are aggregated into fields of monthly/seasonal streamer frequencies.

It should be noted that for interpreting the seasonal frequencies, the seasonal variation in the altitude of

isentropic levels must be considered (see also Wernli and Sprenger, 2007). During winter, at a particular latitude, a specific isentropic surface is located at higher elevations/lower pressure than in summer. As a consequence the intersection of the individual isentrope with the dynamical tropopause and the ground occurs further south during winter. Generally, the intersection of isentropic surfaces with the tropopause is located in the extra-tropics on the lower level and potentially colder isentropes and in the subtropics on the higher level and potentially warmer isentropes. Hence, the terms "extra-tropical isentropes" and "subtropical isentropes" will be used for the lower (colder) and higher (warmer) isentropic levels, respectively.

2.2 *Calculation of the isentropic tropopause variability*

The isentropic dynamical tropopause identified by the PV streamer search algorithm (see previous paragraph) is used to calculate a complementary measure of the synoptic and sub-synoptic scale variability. At every longitude and for every day of the year the variation of the meridional position of the 2-pvu contour about the respective monthly mean latitude is calculated over the ERA-40 period. The standard deviation (STD) about this mean is a measure of the high-frequency variability in the latitude of the tropopause. The monthly mean in the calculations is subtracted to remove any long-term trends. A similar analysis is undertaken for the low frequency latitudinal variability of the dynamical tropopause by calculating the STD of these monthly means. As a crosscheck the statistically robust median absolute deviation, MAD=median(x-median), is calculated for both cases. The results agree very well with those of the STD analysis.

2.3 *Large-scale teleconnection indices*

While the previous analyses are carried out for the entire year, the influence of the large-scale teleconnection patterns on the streamer frequency distribution is studied only for winter months (December, January, February, DJF) when the analyzed patterns are of major importance dynamically. Daily PNA and NAO indices are taken from NOAA's Climate Prediction Center (CPC)(Available from http://cpc.noaa.gov) and are based on the NCEP reanalysis data (Kalnay et al., 1996). All winter days are split into three samples. Two samples comprise all days with an index exceeding one positive or one negative standard deviation, respectively, and the third sample consists of the remaining winter days. Following Trenberth (1997) monthly SST anomalies of the Niño 3.4 region from the CPC are used to define El Niño and La Niña months. The samples are then used to extract streamer composites for low- and high-index states.

A Monte Carlo significance test of the streamer composites is performed for different phases of the teleconnection indices. At each grid-point the percentile in which the observation is located in a 200 member random sample is determined. The random samples are constructed in such a way that the autocorrelation of the indices is taken into account. Points located outside of the two-sided 95% percentile and where the streamer frequency exceeds 0.1% are marked as significant.

2.4 *Comparison of the ERA-40 and ERA-15 PV streamer climatologies*

Wernli and Sprenger (2007) discuss in detail the main characteristics of the spatial and temporal variations in the frequency of stratospheric and tropospheric PV streamers for the ERA-15 period (1979–1993). Their results generally agree very well with the frequency distributions obtained by using the ERA-40 data set. The positions of the frequency maxima are almost perfectly congruent. The frequency distributions found in the ERA-40 data set are spatially smoother compared to those in the ERA-15 climatology. Some differences exist in the amplitudes of the frequencies. These differences are consistent for both stratospheric and tropospheric streamers. The largest discrepancies are found during winter on the isentropes larger than 325 K. Here, the ERA-40 frequencies show substantially smaller amplitudes (up to 50% decrease), and the longitudinal extent of the frequency maxima is less. Potential explanations of these differences are: (1) changes in the low-frequency variability of some phenomenon, such as the ENSO, and/or long-term trends over the ERA-40 period and (2) changes in the data quality and/or data assimilation system, including the forecast model (Uppala et al., 2005).

In a separate study, PV streamer frequency trends have been investigated over the ERA-40 period (Isotta et al., 2008). Both stratospheric and tropospheric PV streamers exhibit positive trends between 330 K and 350 K in the Pacific area and on 330 K and 340 K surfaces in the Atlantic area. The frequencies are therefore higher in the ERA-15 climatology. These trends, however, only partially explain the difference in the streamer frequencies. A further analysis shows that the differences are largest in February over the Atlantic and that the same is true for the wind fields.

The climatology can be compared to and validated against other climatological studies of breaking Rossby waves and PV-intrusions. Climatologies of closely related atmospheric features include, for example, the 10-year data set of breaking Rossby-waves in the northern hemispheric subtropics of Postel and Hitchman (1999), the 20-year climatology of PV intru-

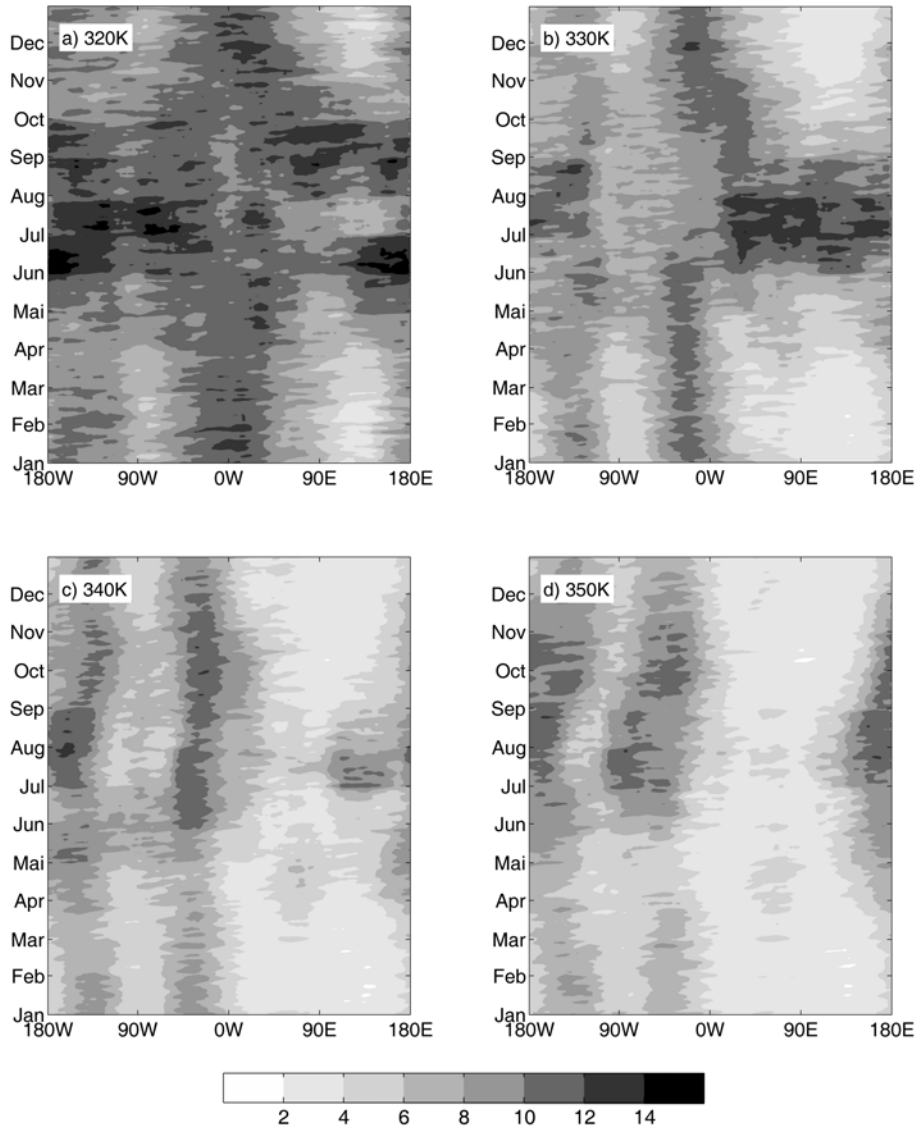

Fig. 1. Hovmöller diagrams of the standard deviation of the latitudinal variation (° shaded) of the isentropic tropopause during the course of the year (see text for further details). (a) on 320 K, (b) on 330 K, (c) on 340 K and (d) on 350 K. The field has been slightly smoothed with a diffusion filter.

sions in the subtropics (350 K) by Waugh and Polvani (2000) and a 40-year climatology of subtropical planetary wave breaking by Abatzoglou and Magnusdottir (2006). Similarities and differences to these climatologies will be discussed in the following sections.

3. Synoptic-scale variability of the isentropic dynamical tropopause

The variability in the latitudinal location of the isentropic dynamical tropopause is presented in the form of Hovmöller diagrams (Fig. 1). This form of analysis allows a compact overview over where (zonally) and when (seasonally) the variability is especially high or low. The variability is a reflection of both the occurrence of (sub) synoptic-scale waves and PV streamers (Martius et al., 2006a). The variability is independent of the specific criteria of the streamer detection algorithm and can, therefore, serve as a cross-check for the general results of the streamer climatology. A comparison to PV streamer counts (Fig. 2) shows that the overall temporal and spatial variation of tropopause variability is very closely reflected in the variations of the streamer frequencies [for a two-dimensional spatial distribution of the ERA-15 PV streamer frequencies see Wernli and Sprenger (2007),

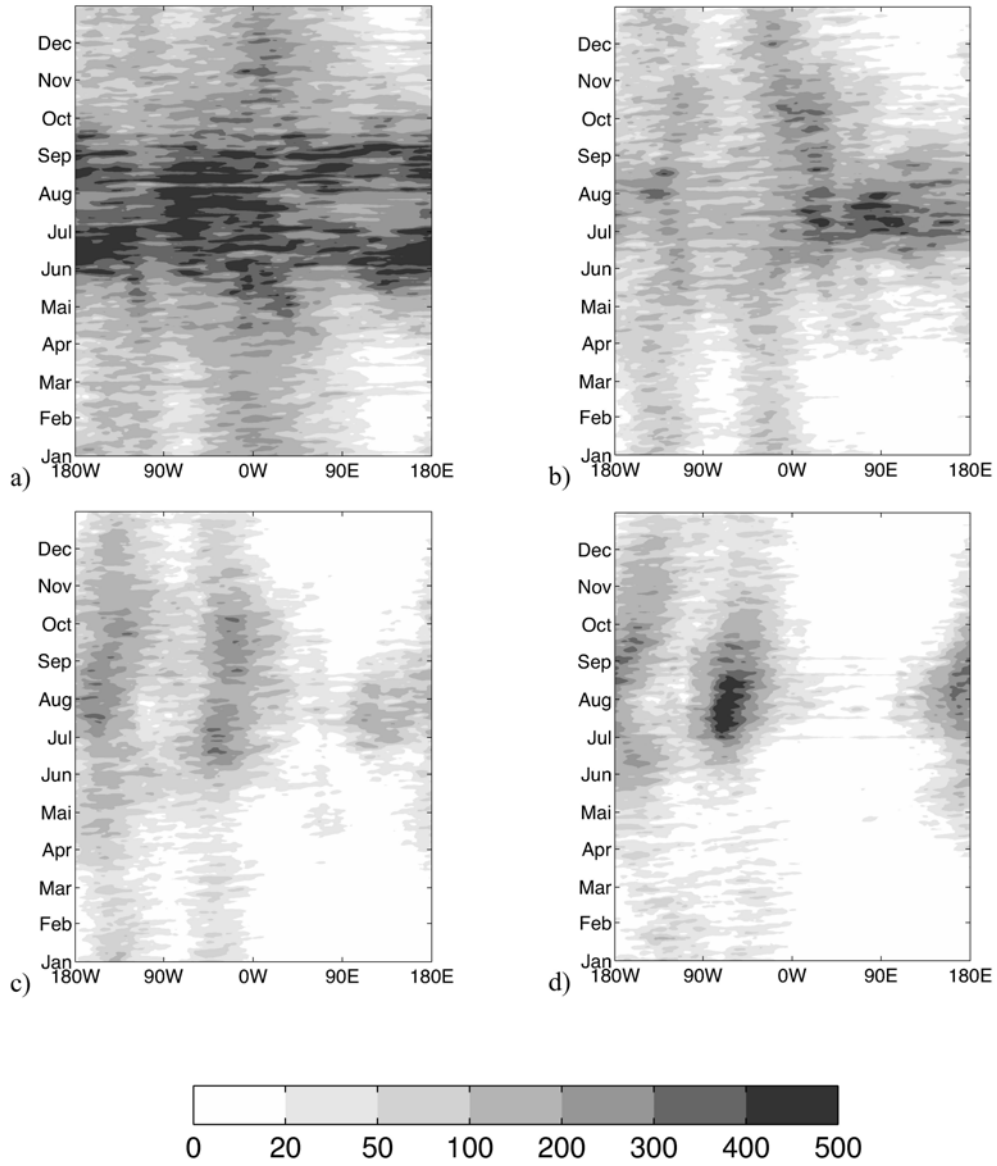

Fig. 2. Hovmöller diagrams of ERA-40 streamer counts (shaded) during the course of the year (see text for further details). (a) on 320 K, (b) on 330 K, (c) on 340 K and (d) on 350 K. The plot has been slightly smoothed with the same filter as Fig. 1.

their Figs. 4 and 6].

On the 320 K isentrope the winter and spring variability and streamer frequency is largest in two clearly separated longitudinal bands (Figs. 1a and 2a) located in the downstream part of the North Pacific (around 170°W) and North Atlantic (around 0°) storm tracks. The stronger maximum in variability is situated over the eastern Atlantic and Western Europe, collocated with the zonal streamer frequency maximum. The second maximum is located over the central and eastern Pacific, and a minimum is found over Eastern Asia. The clear zonal separation into minima and maxima vanishes during summer months and in early autumn when an annular area of increased variability and streamer counts is found. The amplitude of the minimum over the western Pacific (around 145°E) centered in July must be interpreted cautiously. In this summer period the vertical overlap of the tropopause and the 320 K isentrope is very shallow, which could potentially lead to an underestimate of the variability. The isentropic PV-gradients on the 320 K surface in June, July and August (not shown) are increased over the western Pacific in July, indicating that the observed decrease in the number of streamers and the variability is a robust feature.

On the 330 K isentropic surface during winter two

longitudinally contracted maxima in the variability and the streamer counts are found over the eastern Atlantic and the eastern Pacific (Figs. 1b and 2b). Between these maxima the tropopause variability and the streamer counts are very low, especially over the Asian continent. This distribution changes substantially during summer when a zone of increased variability extends from Europe over the Asian continent. This maximum coincides with frequent occurrences of tropospheric and stratospheric PV streamers (Wernli and Sprenger, 2007 and Fig. 2b). During summer the primary distorting mechanism of the tropical, subtropical and extra-tropical tropopause over Asia is the Indian summer monsoon (e.g., Webster et al., 1998). Randel and Park (2006) point out that strong convective events over India lead to a diabatic depletion of the upper-level PV and, hence, a strengthening of the Monsoon anticyclone. As a result, high PV is advected towards lower latitudes along the eastern edge of the Monsoon anticyclone. These features are reflected in an increase in the contour variability and can be detected as PV streamers. A strengthening of the Monsoon anticyclone is accompanied by stronger PV gradients along its northern edge. These act as wave guides and allow the eastward propagation of wave disturbances from wave source regions located over the Mediterranean (Rodwell and Hoskins, 2001; Enomoto et al., 2003) and, hence, lead to an increase of the contour variability. This so-called "Silk road wave pattern" extends far downstream and can influence the Bonin high over Japan.

On the 340 K surface a similarly increased variability of the contours is found over Japan and the western Pacific during July and early August (Figs. 1c and 2c). On this and the 350 K isentrope the variability and streamer counts are low during winter around the entire hemisphere, but show a substantial increase during summer and early autumn over the western Atlantic and the central and eastern Pacific (Figs. 1d and 2d). This agrees well with the observed enhanced frequency of streamers and breaking Rossby waves in these areas (Postel and Hitchman, 1999; Abatzoglou and Magnusdottir, 2006; Wernli and Sprenger, 2007).

An annual minimum of the variability is present on the 350 K surface, primarily over the Atlantic basin in April and early May. This accompanies a clear reduction of PV streamer frequency in this region at this level in spring, as observed in both the ERA-15 and the ERA-40 streamer climatology (not shown). A similar reduction in the number of breaking planetary-scale waves and increase of the PV gradient in the Atlantic basin in spring is found in the NCEP data set (Abatzoglou and Magnusdottir, 2006). This minimum in the variability might be linked to the final breakdown of the polar vortex, which in the climatological mean occurs in mid-April (e.g., Black and McDaniel, 2007). A small and marginally significant increase of the zonal mean zonal wind speed around 35°N is observed during the 10-day period preceding the final stratospheric warming (Black and McDaniel, 2007). This conclusion by analogy, however, is complicated by the fact that the reduction in variability primarily occurs in the Atlantic basin, and the findings of Black and McDaniel (2007) are based on zonal means.

In winter the variability and PV streamer count maximum over Europe and the Atlantic are shifted westward with height by about 50°, from 320 K to 350 K. The reason for this shift lies in the transition from the extra-tropical regime at lower (colder) levels to the subtropical regime at higher (warmer) levels. The forcing mechanisms for the ambient flow are different in the extra-tropics and in the subtropics. While the extra-tropical regime is predominantly forced by baroclinic instability, the subtropical flow is strongly influenced by the Hadley circulation and, hence, susceptible to forcing from the tropics (e.g., Lee and Kim, 2003).

4. Low frequency variability of the dynamical tropopause and PV streamers

4.1 *Inter-annual variability of the dynamical tropopause*

A similar analysis to that presented in section 3 can be undertaken for the inter-annual variability of the dynamical tropopause (not shown). The amplitude of the inter-annual variability amounts to less than a third of that of the short-term variability. In general in areas that exhibit a strong high-frequency variability the inter-annual variability is enhanced as well. In winter the variability maxima are located over the Atlantic and the Pacific ocean, suggesting a link to low-frequency variations of the El Niño Southern Oscillation (ENSO) and the North Atlantic Oscillation (NAO) pattern (e.g., Wanner et al., 2001), respectively. This variability is largest on the coldest (320 K) isentropic level and stronger in the Pacific basin, in marked contrast to the high-frequency variability with the stronger Atlantic maximum. In summer a dominant maximum of variability over Asia extends into the western Pacific. Given its geographic location, this maximum is likely linked to the inter-annual variability of the Indian summer monsoon (Webster et al., 1998). In summary, areas of the dynamical tropopause that experience the strongest variability during winter, both for low and high frequencies, are located in the longitudinal range of the dominant Northern Hemispheric teleconnection patterns. This connection is dis-

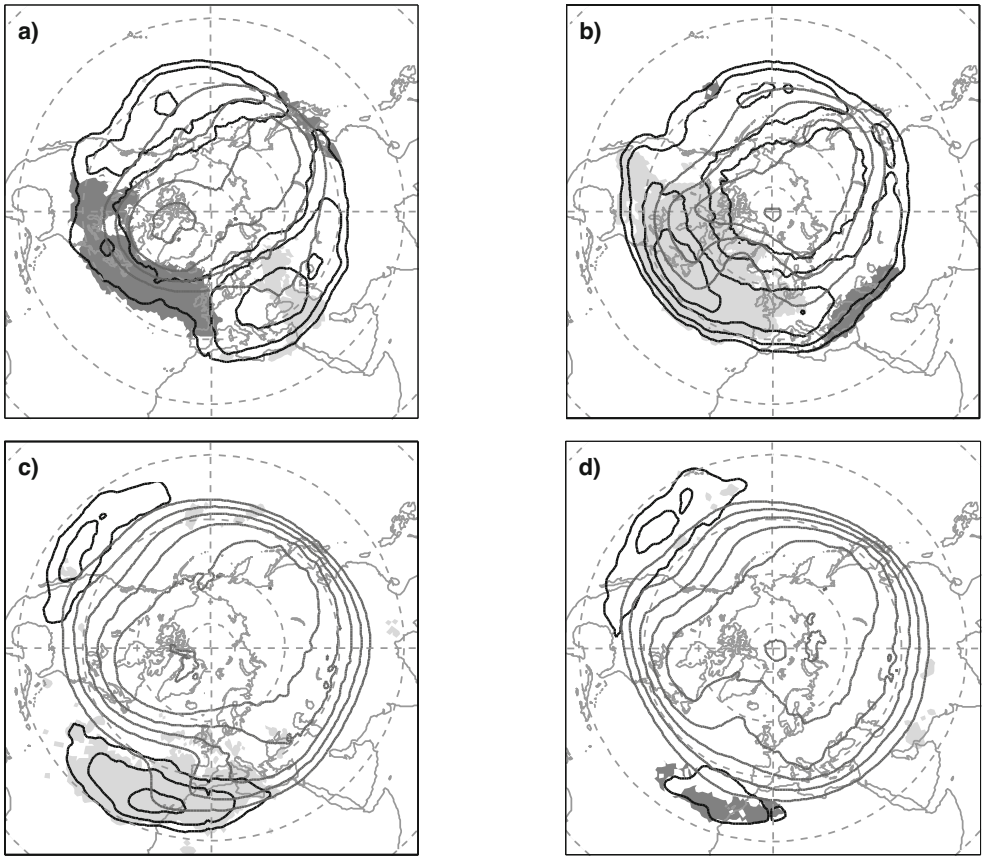

Fig. 3. DJF PV streamer frequencies (a, c) during the positive phase of the NAO and (b, d) during the negative phase (thick solid black lines) (0.25%, 0.5%, 1%, 1.5%, 2%, 3%) on (a, b) 310 K and on (c, d) 330 K, frequencies are relative to the entire time span. Areas where the frequencies are significantly (95%) above (beneath) the climatological distribution are marked with light (dark) grey. The mean isentropic PV distribution during opposed phases is indicated (solid grey lines) (2, 3, 4, 5, 6, 7, 8 PVU).

cussed in more detail in the following sections.

4.2 *Composites for opposed NAO phases*

It has been suggested that the location of the breaking waves over the Atlantic are closely linked to the NAO pattern (see section 1). The changes in streamer frequencies between the positive (NAO+) and negative (NAO−) phases are presented here.

On the lower isentropic surfaces (310 K, 320 K) the stratospheric streamer frequency is significantly reduced across the entire Atlantic basin during NAO+ compared to climatological values, and slightly increased over central Asia (Fig. 3a). The opposite is found during NAO− (Fig. 3b). Stratospheric streamer frequencies with NAO− are significantly above the climatological mean value across the entire Atlantic basin and the eastern North American continent and slightly lower than in the climatological mean over the Mediterranean area and central Asia (Fig. 3b). Tropospheric streamer frequencies generally follow the distribution patterns of the stratospheric streamers, except for a northward shift (∼15°–20°) of the tropospheric PV streamer maxima (not shown). Hence, on 310 K and 320 K surfaces significantly more tropospheric streamers (i.e., low-PV intrusions) occur during NAO− in the area of the low-PV ridge over the northwestern Atlantic and Greenland. This is in good agreement with the observation that blocking is very frequent in this area during NAO− (Croci-Maspoli et al., 2007) and that blocking and tropospheric streamers are observed to frequently coincide. With increasing isentropic levels the frequency of streamers decreases to very low values during NAO− over the entire Atlantic sector (Fig. 3d) and significantly increases during NAO+ over the subtropical central and eastern Atlantic (Fig. 3c). This maximum in the stratospheric PV streamer frequency is co-located with a tongue of high PV extending into the subtropics over West Africa in the mean PV field (Fig. 3c). Tropospheric PV streamers contemporaneously occur more

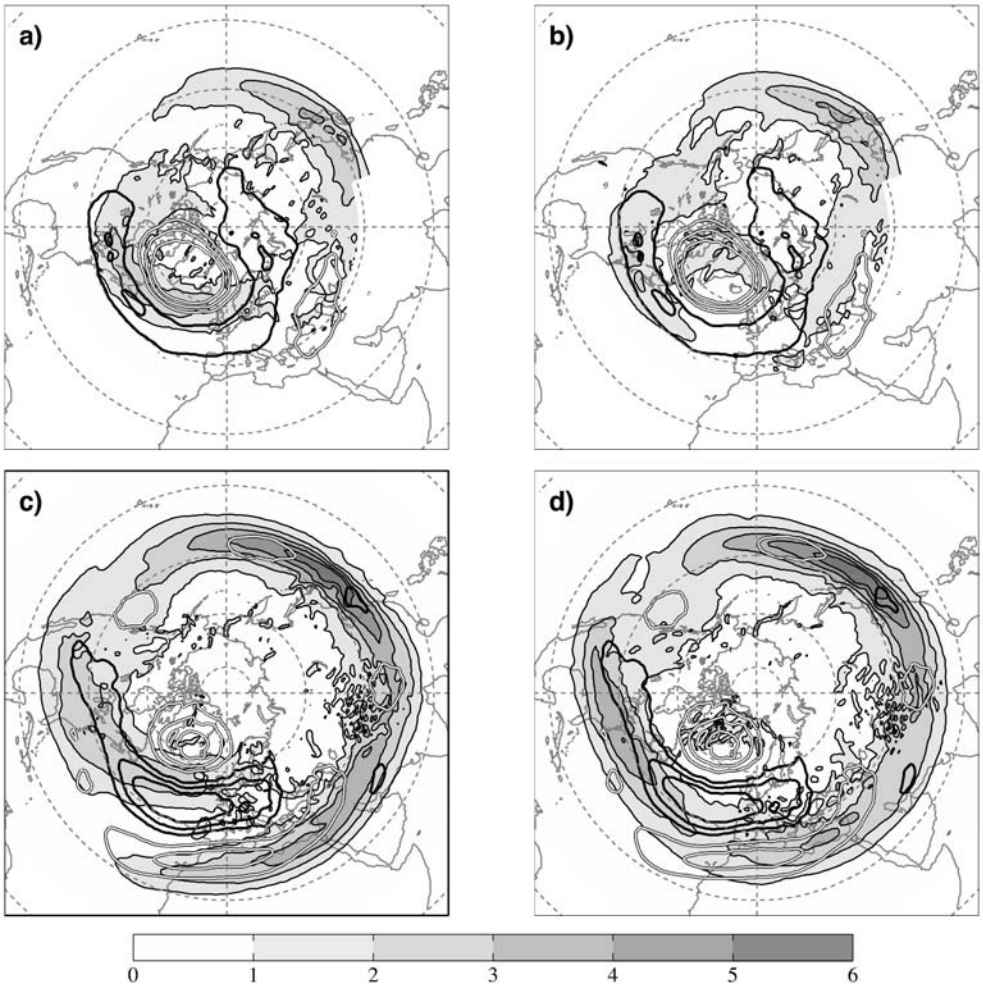

Fig. 4. Isentropic PV-gradients (shaded) (PVU 10^6 m^{-1} and differences in isentropic PV) (NAO+−NAO−, black and white line+, black line−) (−1.2, −0.8, −0.4, 0.4, 0.8, 1.2 PVU) on 310 K (a, b) and on 330 K (c, d) during the positive (a, c) and the negative (b, d) NAO phase. Areas around the Himalayas are cut-out on the low level (a, b).

frequently in the area of the low-PV ridge located upstream over the western Atlantic (not shown).

The isentropic PV distribution in the tropopause region over the Atlantic basin varies substantially between opposite phases of the NAO (Fig. 3), and the location and strength of the isentropic PV gradients change accordingly (Fig. 4). Recall from section 1 that changes in the stratospheric PV streamer frequencies are closely linked to the changes in the mean PV-gradients. PV streamers occur predominantly in locations where the PV gradients are weak. This also holds true during opposite phases of the NAO (Figs. 3 and 4). During NAO+ isentropic PV gradients on 310 K are relatively strong over Newfoundland and the entire northern Atlantic and weak over Europe (Fig. 4a). During NAO− on the other hand, they are stronger over Newfoundland and over northern Greenland (Fig. 4b). The difference in isentropic PV between NAO+ and NAO− has the form of a strong positive pole over Greenland framed by a negative band to the south that extends from the Great Lakes to the Bay of Biscay and into Siberia. Further south a second positive peak is located over the Middle East and central Asia. Qualitatively the differences in PV observed between NAO+ and NAO− match the changes in the frequency of low PV (i.e., tropospheric) and high PV (i.e., stratospheric) streamers very well.

On higher isentropic surfaces and during NAO+ (Fig. 4c) a band of weaker PV gradients is located over the eastern Atlantic, bounded to the north and to the south by strong gradients. This pattern bears a strong resemblance to the typical PV gradient distribution associated with breaking waves, as has been observed in idealized models (McIntyre, 2000 and references therein). With increasingly warmer isentropic surfaces, isentropic PV gradients become significantly

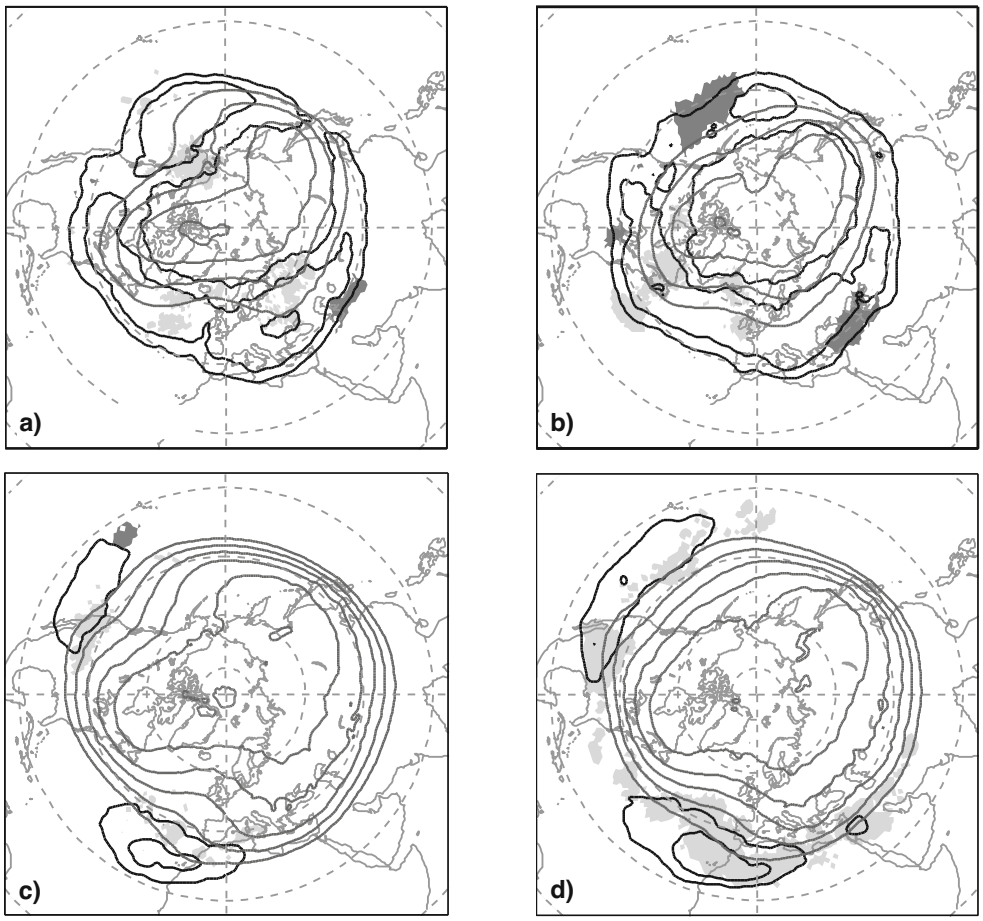

Fig. 5. Same as Fig. 3 but for PNA.

stronger during NAO−. On 330 K a coherent band of strong PV gradients over the Euro-Atlantic sector is only slightly weakened in a small region over the subtropical eastern Atlantic (Fig. 4d). At this level (330 K) the difference in isentropic PV (Figs. 4c and 4d) shows a weaker positive center over Greenland, framed by a stronger negative peak over the central northern Atlantic and a positive pole stretching across the entire subtropical Atlantic into the Middle East. Note the wave pattern of positive and negative anomalies extending along the subtropical jet wave-guide over Asia and into the Pacific.

4.3 *Composites for opposed PNA phases*

The changes in the streamer frequencies during opposite phases of the PNA are less prominent than those for the NAO. On 310 K, tropospheric and stratospheric streamer frequencies are significantly reduced over the eastern Pacific during the negative phase of the PNA (PNA-) (Fig. 5a). Along the east coast of Canada the frequencies are higher than in the climatological mean. An interesting feature is the far-downstream signature of the PNA over Europe and Central Asia. On 330 K the stratospheric and tropospheric streamer frequency over North America is slightly higher than in the climatological mean during PNA− and, also, in a small area during PNA+ (Figs. 5c and 5d). Further areas of significantly higher tropospheric and stratospheric streamer frequencies during PNA− are found over the Atlantic basin west of the African coast.

As with the NAO, changes in streamer frequencies are associated with corresponding changes in the distribution of the PV gradient. A strong isentropic PV gradient extends from eastern Asia across the Date Line into the eastern Pacific on 310 K during PNA+ (Fig. 6a). During PNA− this PV gradient is considerably weaker in the area around the Date Line (Fig. 6b). On the other hand, over the eastern Pacific the PV gradients are relatively weak in general and particularly so during PNA+. Differences of the isentropic PV show a positive anomaly over the central Pacific and a negative anomaly over Alaska. An additional small amplitude positive anomaly is observed over Europe on 310 K. The changes of the PV gradient over

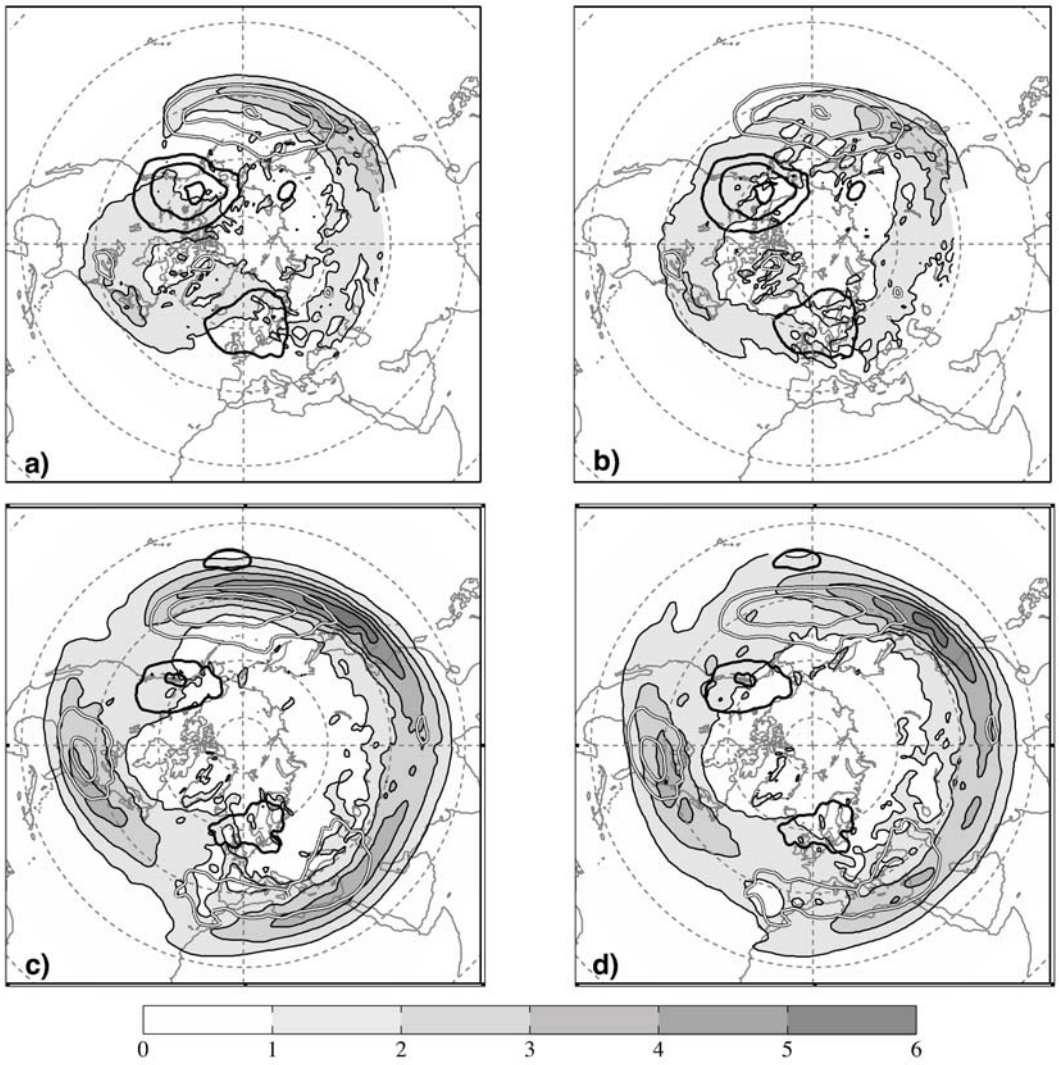

Fig. 6. Same as Fig. 4 but for the PNA.

the central Pacific remain similar with increasing isentropic height up to 330 K (Figs. 6c and 6d). On 330 K the PV difference pattern takes the form of a tripole extending northeastwards from the Date Line. A small amplitude, but large area, positive anomaly is found over the Mediterranean area.

4.4 *Composites for La Niña and El Niño*

The analysis of changes in the stratospheric and tropospheric streamer frequencies during El Niño and La Niña are based on monthly streamer composites. On the lower isentropic surfaces an increase of streamer frequencies is found over the eastern Pacific during El Niño. However, anomalies relative to the climatological streamer frequency are scarcely significant on these surfaces, both in terms of strength and spatial distribution (not shown). On increasingly warmer isentropic levels, streamers are significantly more frequent than in the climatological mean during La Niña over the central subtropical Pacific (Figs. 7a and 7b). This agrees well with the results of Waugh and Polvani (2000), who observe a decrease in the number of stratospheric intrusions in the tropics during the warm ENSO phase in comparison to the cold phase. Over the Atlantic basin a westward shift of the PV streamer maximum takes place during the cold phase.

The changes of the isentropic PV gradients are co-located with changes of PV streamer frequencies. On 340 K stronger PV gradients are present during El Niño to the east of the Date Line (Figs. 7c and 7d) and are collocated with a stronger subtropical jet (Matthews and Kiladis, 1999). Over the central and eastern subtropical Pacific a substantially weaker gradient is found during La Niña, and this gradient is split into a southern and a northern branch (Figs. 7c and

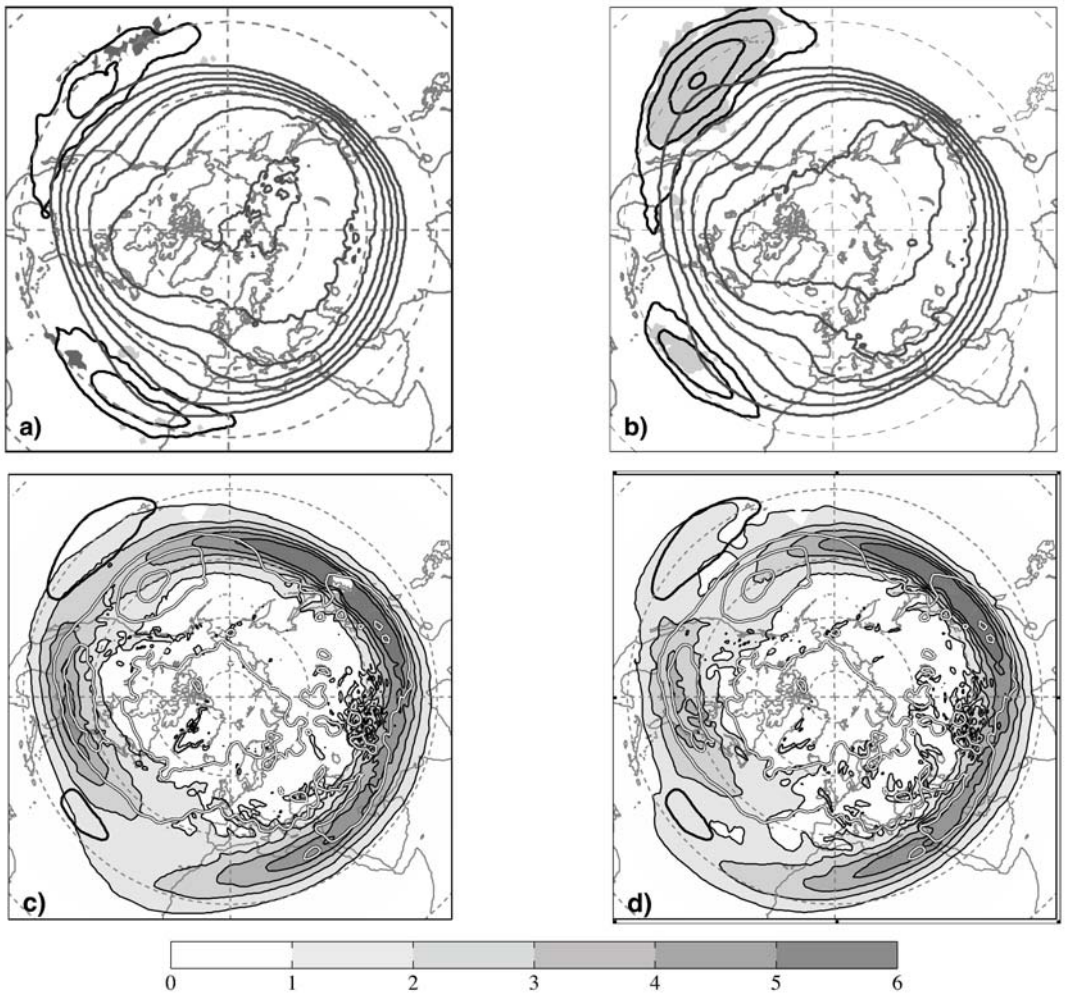

Fig. 7. (a) and (b) DJF PV streamer frequencies during El Niño and La Niña (thick solid black lines) (0.25%, 0.5%, 1%, 1.5%, 2%, 3%). Frequencies are relative to the climate mean. Areas where the frequencies are significantly (95%) above (beneath) the climatological distribution are marked with light (dark) grey. The mean isentropic PV distribution during opposite phases is indicated (grey lines) (2, 3, 4, 5, 6, 7, 8 PVU). (c) and (d) isentropic PV gradients (shaded) (PVU 10^6 m^{-1}) and differences in isentropic PV (El Niño– La Niña, black and white line+, black line −) (−1.2, −0.8, −0.4, 0.4, 0.8, 1.2 PVU), on 340 K during El Niño and La Niña, respectively.

7d) located along the northern and the southern edges of the PV streamer maximum.

5. Summary and discussion

In this paper the inter-annual synoptic-scale and lower-frequency variability of the extra-tropical and subtropical tropopause are discussed from a PV perspective. In the first step variability is defined as the variation in the latitude of the dynamical tropopause on mid-level isentropic surfaces. The seasonal course of this variability on isentropic surfaces ranging from 310 K to 350 K is summarized using Hovmöller diagrams (Figs. 1 and 2) and is linked to the frequency of PV streamers on the same levels. Areas of enhanced variability are co-located with the frequent occurrence of PV streamers (i.e., breaking Rossby waves). In winter, the strongest variability is found on the colder, lower level extra-tropical isentropic surfaces (310 K, 320 K) in the longitudinal range of the North Atlantic and Pacific storm tracks. A maximum is found at their downstream ends, where the baroclinic waves enter the mature non-linear stage of their life cycle and break. Spring is characterized by a very rapid transition from the winter to the summer state, with an absolute annual minimum of the variability over the Atlantic basin on the 350 K surface during April. In summer, the variability of the tropopause is strongly enhanced over the Asian continent on the 330 K surface. This increased contour distortion can be linked to the Asian

summer monsoon. Other areas of large variability are located in the Atlantic and Pacific basin on the 340 K and 350 K surfaces and are closely connected to the subtropical anticyclones (Postel and Hitchman, 1999).

The inter-annual variability of PV streamers is investigated, and possible links to three northern hemispheric teleconnection patterns (NAO, PNA and ENSO) and the large-scale circulation are studied. A general outcome of the analysis of the 44-year PV streamer climatology in the tropopause region is the observation that the climatological mean distribution of PV streamers corresponds closely to the strength of the mean isentropic PV gradients and hence the strength of the mean jet streams. The frequency maxima of the PV streamers are situated in areas where the PV gradients are weak (see also Postel and Hitchman, 1999; Wernli and Sprenger, 2007). This general statement holds true for the climatological distribution, as well as for the flow during both phases of the NAO, PNA and ENSO teleconnection patterns. This link can be interpreted as a two-way interaction between the background state and the breaking waves. Wave breaking is expected to occur in areas where the PV gradients are weaker (see section 1). During wave breaking, the PV gradients are rearranged in a way that an area of weak gradients is located at the center of the breaking wave and is surrounded by strong PV gradients (see McIntyre, 2000 and references therein). Hence an attribution of cause-and-effect to the changes in the large-scale flow during opposite phases of the teleconnection patterns is difficult in the areas where the largest changes in the frequencies of PV streamers are observed.

The amplitude and the location of the PV streamer frequency maxima in the Atlantic basin are closely linked to the NAO teleconnection pattern. The largest frequency differences in amplitude and location are found on the 310 K and 320 K isentropic levels. The frequency of the PV streamers is significantly reduced over the Atlantic Ocean during NAO+ and is increased over the western Atlantic Ocean and North America during NAO−. On higher isentropic surfaces the pattern is exactly the opposite. Streamers are more abundant during NAO+ over the Atlantic basin. These results are in good agreement with the findings of Feldstein (2003), Benedict et al. (2004) and Franzke et al. (2004) who show that the flow during opposite phases of the NAO pattern is characterized by distinct changes of the frequencies of breaking waves in the eastern Pacific and in the Atlantic basin.

As mentioned in section 1, there exists a link between exchange across the tropopause and occurrences of PV streamers. It can be argued that the large amplitude difference and shift in location of PV streamer frequency maxima during opposite phases of the NAO is a likely factor in contributing to the substantial differences between these phases in the observed cross-tropopause exchange during opposite NAO phases (Sprenger and Wernli, 2003).

The PNA-related changes in the PV streamer patterns are smaller than the changes associated with the NAO. At lower levels on colder isentropic surfaces there is an upstream shift of about 20° longitude of the Pacific frequency maximum and a concomitant reduction of the spatial extent of this maximum from positive to negative phases of the PNA. At higher, more subtropical levels on warmer surfaces the differences are even smaller. A large area of significantly increased streamer frequencies is found in the subtropical Atlantic during PNA−. The location of this signal in the subtropics could be an indication of the connectivity of the teleconnection patterns via the circumglobal subtropical wave-guide (Branstator, 2002). A future detailed dynamical investigation of this link between the two ocean basins certainly would be most interesting and valuable.

The influence of the ENSO on the streamer occurrence is mostly confined to the warmer, "subtropical" isentropic levels in the area to the east of the Date Line where the largest changes in the intensity of the subtropical jet are also observed (Matthews and Kiladis, 1999). A significant reduction in the number of streamers is found during the warm ENSO phase. This is in good agreement with the results of Waugh and Polvani (2000). A small eastward shift of the Atlantic streamer maximum is found during the warm phase.

The above summary demonstrates the close links between tropopause variability and the occurrence of breaking waves in the tropopause region and between various processes ranging from the tropics over the stratosphere to the extra-tropical troposphere. Continuing studies towards an integrated picture of these individual influences on the tropopause variability, their relative importance and interaction would be of great value.

Acknowledgements. We would like to thank MeteoSwiss for granting access to the ERA-40 data set. Cordial thanks go to Heini Wernli for the provision of the streamer detection routine. Helpful comments from Mike Blackburn and Rob Black were greatly appreciated. Two anonymous reviewers helped to considerably improve the clarity of this manuscript. This research is supported by the NCCR-Climate program.

REFERENCES

Abatzoglou, J. T., and G. Magnusdottir, 2006: Planetary wave breaking and nonlinear reflection: Seasonal cy-

cle and interannual variability. *J. Climate*, **19**, 6139–6152.

Appenzeller, C., and H. C. Davies, 1992: Structure of Stratospheric Intrusions into the Troposphere. *Nature*, **358**, 570–572.

Benedict, J. J., S. Lee, and S. B. Feldstein, 2004: Synoptic view of the North Atlantic Oscillation. *J. Atmos. Sci.*, **61**, 121–144.

Black, R. X., and B. A. McDaniel, 2007: The Dynamics of the Northern Hemisphere Stratospheric Final Warming Events. *J. Atmos. Sci.*, **64**, 2932–2946.

Branstator, G., 2002: Circumglobal teleconnections, the jet stream waveguide, and the North Atlantic oscillation. *J. Climate*, **15**, 1893–1910.

Croci-Maspoli, M., C. Schwierz, and H. C. Davies, 2007: Atmospheric Blocking-Space-time links to the NAO and PNA. *Climate Dyn.*, DOI 10.1007/s00382-007-0259-4.

Enomoto, T., B. J. Hoskins, and Y. Matsuda, 2003: The formation mechanism of the Bonin high in August. *Quart. J. Roy. Meteor. Soc.*, **129**, 157–178.

Feldstein, S. B., 2003: The dynamics of the NAO teleconnection pattern growth and decay. *Quart. J. Roy. Meteor. Soc.*, **129**, 901–924

Franzke, C., S. Lee, and S. B. Feldstein, 2004: Is the North Atlantic Oscillation a breaking wave? *J. Atmos. Sci.*, **61**, 145–160.

Hoskins, B. J., 1991: Towards a PV-Theta View of the General-Circulation. *Tellus A*, **43**, 27–35.

Hoskins, B. J., M. E. McIntyre, and A. W. Robertson, 1985: On the Use and Significance of Isentropic Potential Vorticity Maps. *Quart. J. Roy. Meteor. Soc.*, **111**, 877–946.

Isotta, F., O. Martius, M. Sprenger, and C. Schwierz, 2008: Long-term trends of synoptic-scale breaking Rossby waves in the northern hemisphere between 1958 and 2001. *International Journal of Climatology*, DOI 10.1002/joc.1647.

Kalnay, E., and Coauthors, 1996: The NCEP/NCAR 40-year reanalysis project. *Bull. Amer. Meteor. Soc.*, **77**, 437–471.

Knippertz, P., and J. E. Martin, 2005: Tropical plumes and extreme precipitation in subtropical and tropical West Africa. *Quart. J. Roy. Meteor. Soc.*, **610**, 2337–2365.

Lee, S. and H. K. Kim, 2003: The dynamical relationship between subtropical and eddy-driven jets. *J. Atmos. Sci.*, **60**, 1490–1503.

Martius, O., C. Schwierz, and H. C. Davies, 2006a: A refined Hovmöller diagram. *Tellus*, **58A**, 221–226.

Martius, O., C. Schwierz, and H. C. Davies, 2006b: Episodes of Alpine Heavy Precipitation with an Overlying Elongated Stratospheric Intrusion: A Climatology. *International Journal of Climatology*, **26**, 1149–1164.

Martius, O., C. Schwierz, and H. C. Davies, 2007: Breaking waves at the Tropopause in the wintertime Northern Hemisphere: Climatological analyses of the orientation and the theoretical LC1/2 classification. *J. Atmos. Sci.*, **64**, 2576–2592.

Massacand, A. C., H. Wernli, and H. C. Davies, 1998: Heavy precipitation on the Alpine southside: An upper-level precursor. *Geophys. Res. Lett.*, **25**, 1435–1438.

Matthews, A. J. and G. N. Kiladis, 1999: Interaction between ENSO, Transient Circulation, and Tropical Convection over the Pacific. *J. Climate*, **12**, 3062–3086.

McIntyre, M. E., 2000: *Perspectives in Fluid Dynamics, A collective Introduction to Current Research*. Cambridge University Press, 631pp.

Postel, G. A., and M. H. Hitchman, 1999: A climatology of Rossby wave breaking along the subtropical tropopause. *J. Atmos. Sci.*, **56**, 359–373.

Randel, W. J., and M. Park, 2006: Deep convective influence on the Asian summer monsoon anticyclone and associated tracer variability observed with AIRS. *J. Geophys. Res.*, **111**, doi:10.1029/2005JD006490.

Rodwell, M. J., and B. J. Hoskins, 2001: Subtropical Anticyclones and Summer Monsoons. *J. Climate*, **14**, 3192–3211.

Shapiro, M. A., H. Wernli, N. A. Bond, and R. Langland, 2001: The influence of the 1997–99 El Niño Southern Oscillation on extratropical baroclinic life cycles over the eastern North Pacific. *Quart. J. Roy. Meteor. Soc.*, **127**, 331–342.

Sprenger, M., and H. Wernli, 2003: A northern hemispheric climatology of cross-tropopause exchange for the ERA15 time period (1979–1993). *J. Geophys. Res.*, **108**, doi: 10.1029/2002JD002636.

Sprenger, M., H. Wernli, and M. Bourqui, 2007: Stratosphere-troposphere exchange and its relation to potential vorticity streamers and cutoffs near the extratropical tropopause. *J. Atmos. Sci.*, **64**, 1587–1602.

Swanson, K. L., P. J. Kushner, and I. M. Held, 1997: Dynamics of barotropic storm tracks. *J. Atmos. Sci.*, **54**, 791–810.

Thorncroft, C. D., B. J. Hoskins, and M. F. McIntyre, 1993: Two paradigms of baroclinic-wave life-cycle behavior. *Quart. J. Roy. Meteor. Soc.*, **119**, 17–55.

Trenberth, K. E., 1997: The Definition of El Niño. *Bull. Amer. Meteor. Soc.*, **78**, 2771–2777.

Uppala, M., and Coauthors, 2005: The ERA-40 reanalysis. *Quart. J. Roy. Meteor. Soc.*, **131**, 2961–3012.

Wanner, H., S. Brönnimann, C. Casty, D. Gyalistras, J. Luterbacher, C. Schmutz, D. B. Stephenson, and E. Xoplaki, 2001: North Atlantic Oscillation-Concepts and Studies. *Surveys in Geophysics*, **22**, 321–382.

Waugh, D. W., and L. M. Polvani, 2000: Climatology of intrusions into the tropical upper troposphere. *Geophys. Res. Lett.*, **27**, 3857–3860.

Waugh, D. W. and B. M. Funatsu, 2003: Intrusions into the tropical upper troposphere: Three-dimensional structure and accompanying ozone and OLR distributions. *J. Atmos. Sci.*, **60**, 637–653.

Webster, P. J., V. O. Magaña, J. Shukla, R. A. Tomas, M.

Yanai, and T. Yasunari, 1998: Monsoons: Processes, predictability, and the prospects for prediction. *J. Geophys. Res.*, **103**, 14,451–14,510.

Wernli, H., and C. Schwierz, 2006: Surface cyclones in the ERA40 Dataset (1958–2001). Part I: Novel identification method and global climatology. *J. Atmos. Sci.*, **63**, 2486–2507.

Wernli, H., and M. Sprenger, 2007: Identification and ERA-15 climatology of potential vorticity streamers and cutoffs near the extratropical tropopause. *J. Atmos. Sci.*, **64**, 1569–1586.